RSC Advances

ROYAL SOCIETY OF CHEMISTRY

www.rsc.org/advances

STUDY OF ELECTRONIC PROPERTIES, STABILITIES AND MAGNETIC QUENCHING OF MOLYBDENUM DOPED GERMANIUM CLUSTER: A DENSITY FUNCTIONAL INVESTIGATION

Ravi Trivedi, Kapil Dhaka, and Debashis Bandyopadhyay*

Department of Physics, Birla Institute of Technology and Science, Pilani, Rajasthan-333031, India

*debashis.bandy@gmail.com

ABSTRACT

Evolution of electronic structures, properties and stabilities of neutral and cationic molybdenum encapsulated germanium clusters ($Mo@Ge_n$, n= 1 to 20) has been investigated using linear combination of atomic orbital density functional theory method with effective core potential. From the variation of different thermodynamic and chemical parameters of the ground state clusters during the growth process, the stability and electronic structure of the clusters is explained. From the study of the distance dependence nucleus independent chemical-shifts (NICS) we found that $Mo@Ge_{12}$ with hexagonal prism like structure is the most stable isomer possesses strong aromatic character. Density of states (DOS) plots of different clusters is then discussed to explain the role of d-orbitals of Mo atom in the hybridization. Quenching of the magnetic moment of Mo atom with the increase of the size of the cluster is also discussed. Finally, the validity of 18-electron counting rule is applied to further explain the stability of the metalloinorganic magic cluster $Mo@Ge_{12}$ and then the possibility of Mo-based cluster assembled materials has been discussed.

Keywords: Clusters and nanoclusters, Binding energy, Density functional theory, Electron affinity, Embedding Energy, Ionization potential, DOS, NICS

1. INTRODUCTION

The number of electrons involved in the growth of the nanoclusters and cluster-assembled materials by forming chemical bonds is the fundamental concept to explain and understand the electronic properties and stabilities of the nanomaterials. In last few decades, searching of stable hybrid nanoclusters, specially, transition metal-doped semiconductor nanoclusters are extremely active area of research for their potential applications in nanoscience and nanotechnology. One of the challenges in the computational materials design or synthesis of such materials is to search for the clusters that are likely to retain their properties and structural reliability during the formation of cluster assembled materials [1]. Among these materials, in the transitional metal-doped semiconductor clusters and cluster-assembled materials are interesting and also it is important to understand the physical and chemical processes taking places at the metal-semiconductor interface for their application as nano-devises [2]. Pure semiconductor nanoclusters are not really stable and it is a challenging job to make them stable. Among different possibilities of stabilizing the semiconductor nanoclusters, encapsulation of a transition metal (TM) in pure semiconductor cage is one of the most effective methods. Many insights of the transition metal doped Si and Ge clusters were reported in literature and also explained their stabilities on the basis of electron counting rules [3-11]. The existence of several stable transition metal doped semiconductor nanoclusters have already experimentally verified by Beck et. al. [12,13] using lasers vaporization techniques. Recently, Atobe et. al. [14] investigated the electronic properties of transition metal and lanthanide-metal doped $M@Ge_n$ (M = Sc, Ti, V, Y, Zr, Nb, Lu, Hf, and Ta) and $M@Sn_n$ (M = Sc, Ti, Y. Zr, and Hf) by anion photoelectron spectroscopy and explained the stability of the clusters using electron-counting rule. In a theoretical study Hiura et. al. [15] argued that the magic nature of $W@Si_{12}$ cluster is because of the 18 electron shell fill structure assuming each silicon atom donates one valence electron to the encapsulated transition metal which is donating six valance electron in hybridization. Wang et. al. [16] found that the encapsulation of Zn atom in germanium cage starts from n=10 whereas, $ZnGe_{12}$ is the most stable species which is not a 18-electron cluster. In another study Guo et. al. [17] explained the stability of $M@Si_n$ (M=Sc, Ti, V, Cr, Mn, Fe, Co, Ni, Cu, Zn; n=8–16) nanoclusters using shell filling model where the d-shell of the transition metals plays an important roll in hybridization to make a closed shell structure. In this context, more corrected information were reported by Revelese and Khanna [18, 19]. They considered that the valence electrons in TM-Si clusters behave like a nearly free-electron gas and one needs to invoke the Wigner-Witmer (WW) spin conservation rule [19] while calculating the embedding energy of the clusters to explain its stability. It is worth mentioning here that the one-

electron levels in spherically confined free-electron gas follow the sequence $1S^2 1P^6 1D^{10} 2S^2$.... Thus, 2, 8, 18, 20, etc. are the shell filling numbers, and clusters having these numbers of valence electrons attain enhanced stability. But in some cases this theory is not valid. As example, by applying Wigner-Witmer (WW) spin conservation rule [19] and without applying that Revelese and Khanna [18, 19] found that $CrSi_{12}$ and $FeCr_{12}$ in neutral state exhibit highest binding energy, whereas, anionic $MnSi_{12}$, VSi_{12} and $CoSi_{12}$ show maximum embedding energy which is one of the most important parameter to understand the stability of the nanoclusters. Therefore, both 18- and 20-electron counting rules are valid for different clusters and in different charged states to explain the stability. Experiments also supported the validity of these electron-counting rules in some of the charged clusters. Koyasu et al. [20] studied the electronic and geometric structures of transition metal (Ti, V and Sc) doped silicon clusters in neutral and different charged states by mass spectroscopy and anion photoelectron spectroscopy. They found that the neutral $Ti@Si_{16}$, cationic $V@Si_{16}$ and anionic $Sc@Si_{16}$ clusters were produced in greater abundance, which follows the validity of 20-electron counting rule. In summary, it was found that in most of the research transition metal-doped semiconductor clusters show maximum stability in closed-shell electron configuration with 18 and 20 valence electrons in the cluster by taking into account the fact that each germanium or silicon atoms contributes one electron to the bonding with the transition metal atom. In the present study we make an effort to explain the enhanced stability of $MoGe_{12}$ in $Mo@Ge_n$ (n=1-20) by following the behavior of different physical and chemical parameters of the ground state clusters in each size using density functional theory (DFT). Detailed studies on this system are important to understand the science behind the cluster stability and its electronic properties. DOS plots of different clusters are also discussed to explain the role of d-orbitals of Mo atom in the hybridization and in the quenching of magnetic moment of Mo atom in germanium cluster. In addition, to understand the enhance stability of $MoGe_{12}$ isomer, distance dependence nucleus independent chemical-shift (NICS), which is the measure of the aromaticity of the cluster is calculated and discussed its role in stability. Finally, electron-counting rule is applied to understand the stability of the $Mo@Ge_{12}$ cluster and the possibility of Mo-based cluster assembled materials.

2. THEORETICAL METHOD ANS COMPUTATIONAL DETAILS

All calculations were performed within the framework of linear combination of atomic orbital's density functional theory (DFT). The exchange-correlation potential contributions are incorporated into the calculation using the spin-polarized generalized gradient approximation (GGA) proposed by Lee, Yang and Parr popularly known as B3LYP

[21]. Different basis sets were used for germanium and molybdenum with effective core potential using Gaussian'03 [22] program package. The standard LanL2DZdp and LanL2DZ basis sets were used for germanium and Molybdenum to express molecular-orbitals (MOs) of all atoms as linear combinations of atom-centered basis functions. LanL2DZdp. This is a double-ζ, 18-valence electron basis set with a LANL effective core potential (ECP) and with polarization function [23-24]. All geometry optimizations were performed with no symmetry constraints. During optimization, it is always possible that a cluster with particular guess geometry can get trapped in a local minimum of the potential energy surface. To avoid this, we used global search method by using USPEX [25] and VASP [26, 27] to get all possible optimized geometric isomers in each size from n=5 to 20. The optimized geometries were then again optimized in Gaussian'03 [22] program using different basis sets as mentioned above to understand the electronic structures. In order to check the validity of the present methodology, a trial calculation is carried out on Ge-Ge, Ge-Mo and Mo-Mo dimers using different methods and basis sets. Detailed result of the out puts is presented in Table 1. The bond length of germanium dimer at triplet spin state (ground state) is found 2.44Å (with a lowest frequency of 250 cm^{-1}) in the present calculation, which is within the range of the values obtained theoretically as well as experimentally reported by several groups (see Table 1). The bond length and the lowest frequency of the Ge-Mo dimer in the quintet spin state (ground state) were obtained in the present calculation as 2.50 Å and 207.82 cm^{-1} respectively. The values reported by other groups are 2.50 Å and 208 cm^{-1} as shown in Table 1. The optimized electronic structure is obtained by solving the Kohn-Sham equations self-consistently [33] using the default optimization criteria of the Gaussian'03 program [22]. Geometry optimizations were carried out to a convergence limit of 10^{-7} Hartree in the total optimized energy. The optimized geometries as well as the electronic properties of the clusters in each size were obtained from the calculated program output.

Table 1. BOND LENGTH AND LOWEST FREQUENCIES OF GE-GE, GE-MO AND MO-MO DIMERS

Dimer	Bond length (Å)	Lowest frequencies (cm^{-1})
Ge-Ge	2.44[a], 2.44[b], 2.44[c], 2.39[d], 2.3[e], 2.36-2.42 [28, 29], 2.46 [32]	250.63[a], 261[b], 263[c], 282[d], 317.12[e], 258 [28]
Ge-Mo	2.5[a], 2.48[b], 2.51[c], 2.41[d], 2.43[e], 2.50 [29]	202.56[a], 218[b], 198[c], 251.78[d], 252.53[e], 287.82 [29]
Mo-Mo	1.97[a], 2.5[b], 2.5[c], 1.88[d], 1.89[e], 1.98 [30]	561.79[a], 567.24[b], 570.36[c], 582.1[d], 583.07[e], 562 [30], 477 [31]

[a] B3LYP/Lanl2dz-ECP, [b] B3LYP/aug-cc-pvdz, [c] B3LYP/aug-cc-pvtz-pp, [d] M06/aug-cc-pvtz-pp
[e] M06/Lanl2dz-ecp

3. RESULTS AND DISCUSSIONS

Molybdenum atom, a typical 4d transition metal, has electronic configuration of $[Kr]4d^5 5s^1$ where 'd' and 's', both the shells are half filled. Optimized ground state clusters with the point group symmetry are shown in supplementary information Fig. 1SIa. Following the growth pattern of Ge_nMo clusters from n=1 to 10, the Mo is absorbed on the surface of the Ge_n cluster or replace a Ge atom from the surface of Ge_{n+1} cluster to form Ge_nMo cluster where Mo atom in all clusters are exposed outside. In the next stage of the growth pattern, Mo is absorbed partially by the Ge_n clusters in n=8 and n=9. Complete encapsulation starts from n=10. The low energy structures within the size range n = 10 to 16 are all very known in most of the transition metal doped silicon and germanium clusters and also reported by others [34-38]. The first encapsulated ground state isomer $Mo@Ge_{10}$ is icosahedral, where, the Mo atom makes hybridization with all ten-germanium atoms in the cage. Addition of one germanium atom on the surface of ground state $Mo@Ge_{10}$ isomers gives endohedral Mo doped $Mo@Ge_{11}$ cluster. Endohedrally absorbed Mo in hexagonal prism kind structure $Mo@Ge_{12}$ is the ground state isomer at n=12 size. Here Mo bonded with all twelve germanium atoms in the cage. In this structure Mo atom is placed between two parallel benzene likes hexagonal Ge_6 surfaces. The ground state isomer of $Mo@Ge_{13}$ structure is a Mo encapsulated hexagonal capped bowl kind of structure. The structure can be understood by capping one germanium atom with the hexagonal plane of n=12 ground state isomer. The ground state structure of $Mo@Ge_{14}$ is a combination of three rhombus and six pentagons, where, rhombuses are connected only with the pentagons. It is a threefold symmetric structure. The other bigger structures can be understood by adding a single Ge or a Ge-Ge dimer with the lower sizes. In all ground state Ge_nMo clusters from n=10 to 14, Mo atoms takes an interior site of the Ge_n cage and make the cages more symmetric compare to the pure Ge_n cages. This continued up to the end size rage in the present study. Among all these nanoclusters between $8 \leq n \leq 20$, the ground state $Mo@Ge_{12}$ is the most symmetric.

3.1. ELECTRONIC STRUCTURES AND STABILITIES OF $Mo@Ge_n$ NANOCLUSTERS

We first studied the energetic of pure Ge_n and $Mo@Ge_n$ clusters. Then we explored the electronic properties and stabilities of the $Mo@Ge_n$ clusters, by studying the variation of different thermodynamic parameters of the clusters, like, average binding energy (BE), embedding energy (EE), fragmentation stability (ΔE) and second order change in energy (Δ_2) with the increase of the cluster size following the reported work [7-11]. The average binding energy per atom of $Mo@Ge_n$ clusters here is defined as:

$$BE = \left(E_{Mo} + nE_{Ge} - E_{Mo@Ge_n}\right) \Big/ \left(n+1\right)$$

and by definition it is always positive. The variation of the binding energy of the clusters with the cluster size is presented in Fig.1. For pure germanium clusters E_{Mo} in the above equation is taken as zero and n+1 is replaced by n. Following the graphs, the binding energy of small sized clusters in the size range from 1 to 5 increases rapidly. This is an indication of thermodynamic instability of these clusters (both pure and doped Ge_n). For the sizes n>5 the binding energy curve increase with relatively slower rate. Binding energy of the Mo doped clusters is always higher than the same size pure germanium cluster for n>6 indicate that the doping of transition metal atom helps to increase the stability of the clusters. It is to be noted that there are two local maxima in the binding energy graph at n=12 and 14. According to the 18- or 20-electron counting rule, the binding energy and other thermodynamic parameter should show a local maxima (or minima) at n=12 and 14 for neutral clusters respectively. Other 18 and 20 electron clusters are at n=13 and 15 in cationic and n=11 and 13 in anionic states assuming each germanium atom is contributing one valance electron in the hybridization with the Mo following our previous work [10]. Following the Fig.1, the behaviour of the neutral and anionic clusters is same and both of them show a peak at n=12 in the binding energy graph. However, the cationic cluster shows a peak at n=11 and it follows the demand of the 18-electron counting rule. Because of the anomalous behaviour of the anionic clusters, in the present study we considered only neutral and cationic clusters. Another important parameter that explains thermodynamic stability of the nanoclusters is embedding energy (EE). In the present study, the embedding energy of a cluster after imposing Wigner-Witmer spin-conservation rule [19] is defined as:

$$EE^{WW} = E\left({}^{M}Ge_n\right) + E\left({}^{0}Mo\right) - E\left({}^{M}Ge_nMo\right)$$

or,

$$EE^{WW} = E\left({}^{0}Ge_n\right) + E\left({}^{M}Mo\right) - E\left({}^{M}Ge_nMo\right)$$

where, M is the total spin of the cluster or the atom in units of $h/2\pi$. Following this definition EE is positive, which means addition of transition metal atom to the cluster, is favorable. In the above embedding energy expressions, we have chosen the higher of the resulting two EEs. In the present calculation, ground states for n=1 and 2 are quintet and triplet respectively. For n>2, all ground states are in singlet state. Therefore, to calculate the EE according to the

WW spin-conversation rule, pure Ge clusters were taken to be in either the triplet or the singlet state. For cationic $Mo@Ge_n$ clusters the EE can be written as:

$$EE^{WW} = E\left({}^{M}Ge_n^{\pm}\right) + E\left({}^{0}Mo\right) - E\left({}^{M}Ge_nMo^{\pm}\right)$$

or,

$$EE^{WW} = E\left({}^{0}Ge_n\right) + E\left({}^{M}Mo^{\pm}\right) - E\left({}^{M}Ge_nMo^{\pm}\right)$$

Variation of EE and ionization potential with the size of cluster is shown in Fig. 2a. Both neutral and cationic clusters show maxima at n=12 and 13 respectively. Both the clusters are 18-electron clusters. To check weather the neutral and cationic clusters are following 20-electron counting rule, we studied the BE and EE values at n=14 and 15. In the BE graph, at n=14, there is no relative maxima. At n=14, EE shows a local minima. Hence it clearly shows that n=14 ground state cluster does not follow 20-electron counting rule. To further check the stability of the clusters during the growth process by adding germanium atom one by one to Ge-Mo dimer, 2nd order difference in energy (Δ_2 or stability) and the fragmentation energy (FE), Δ(n,n-1) are calculated following the relations given below:

$$\Delta(n,n-1) = -\left(E_{Ge_{n-1}Mo} + E_{Ge} - E_{Ge_nMo}\right)$$

$$\Delta_2(n) = -\left(E_{Ge_nMo} + E_{Ge_{n-1}Mo} - 2E_{Ge_nMo}\right)$$

means, higher positive values of these parameters indicate the higher stability of the clusters compare to its surrounding clusters during growth process. Variations of fragmentation energy and stability with the size for neutral and cationic clusters are shown in Figs. 2b and 2c respectively. The sharp rise in FE from n=11 to 12 and sharp drop in the next step from n=12 to 13 during growth process indicates that in neutral state $Mo@Ge_{12}$ size is favorable compare to its neighboring sizes. The same is true for cationic clusters at n=13. This is an indication of higher stability of neutral $Ge_{12}Mo$ and cationic $Ge_{13}Mo$ clusters. There is a sharp rise in Δ_2 when 'n' changes from 11 to 12 and from 12 to 13 in neutral and cationic states respectively as shown in Fig. 2c. This is an indication of higher stability of the clusters at n=12 and 13 in neutral and cationic states respectively. Drastic drop in Δ_2 from n=12 to 13 in neutral and from n=13 to 14 in cationic clusters respectively are again indication of the enhanced stability of these clusters. Both of these parameters are again supporting the enhanced stability of ground state neutral n=12 and cationic n=13 clusters during the growth process and follow 18-electron counting rule. The binding energy of the

clusters, both in pure Ge_n and Ge_nMo, first increases rapidly and then saturates with a small fluctuation. However, the variation of Δ_2 and Δ, is oscillatory in nature. We also measured the gain in energy in pure germanium clusters. The gain in energy (2.83 eV) in pure Ge_{13} cluster is higher than Ge_{12} (2.68 eV) and Ge_{14} (2.80 eV). The gain in energy is even more in doped clusters. For $Ge_{11}Mo$, $Ge_{12}Mo$ and $Ge_{13}Mo$ these values are 2.33 eV, 3.13 eV and 2.30 eV respectively. Though the FE and stability are oscillatory in nature, but from the systematic behaviour of these two parameters at n=12 (neutral) and 13 (cationic) sizes we can take these two 18-electron clusters as the most stable clusters in the neutral and cationic $Mo@Ge_n$ series. Therefore, it is clear that BE, EE, FE and Δ_2 (n) parameters support relatively higher thermodynamic stability of $Mo@Ge_{12}$ in neutral and $Mo@Ge_{13}$ in cationic states where both the clusters have closed shell filled 18-electron structure.

To understand the stability of the $Ge_{12}Mo$ cluster we further studied the charge exchange between the germanium cage and the embedded Mo atom in hybridization during the growth process using Mulliken charge population analysis and shown in Electronic Supplementary Information Fig. 2SI. As like the other thermodynamic parameters, the charge on the Mo and Ge atoms show a global maximum and minimum respectively at n = 12. The electronic charge transfer is always from germanium cage to Mo atom in different $Mo@Ge_n$ clusters. In the figure the charge on Mo is plotted in units of 'e', the electronic charge. Since the average charge per germanium atom and the charge on molybdenum atom in $Ge_{12}Mo$ cluster are minimum and maximum respectively, therefore the electrostatic interaction increases and hence improve the stability of $Ge_{12}Mo$ cluster. The effect of ionization (neutral to cation or anion of n=12 ground state) that gives redistribution of electronic charge density in the orbitals can be seen from the orbital plot in Electronic Supplementary Information Fig. 1SIb. With reference to the Fig.1SIb, addition of one electron to $Ge_{12}Mo$ neutral cluster, the higher order orbitals just shifts to one step down and holds the orbitals similar to the neutral cluster. As example, the HOMO, LUMO and LUMO+1 orbitals of neutral $Ge_{12}Mo$ shifts to anionic $Ge_{12}Mo$ HOMO-1, HOMO and LUMO respectively. However, the HOMO and LUMO orbitals remains unchanged when neutral $Ge_{12}Mo$ cluster ionized to cationic cluster. Details of the natural electronic configuration (NEC) for $Ge_{12}Mo$ ground state cluster is shown in Table 2. Combining the Fig. 2SI in Electronic Supplementary Information and Table 2, it is seen that when the charge transfer takes place between the germanium cage and the Mo atom, at the same time there is rearrangement of electronic charge in 5s, 4p and 4d orbitals in Mo; and 3d, 4s and 4p orbitals of Ge to make the cluster stable. According to the Table 2, the main change contribution in hybridization between Mo and Ge are from d-orbitals of Mo and s, p orbitals of Ge atoms in the ground state $Mo@Ge_{12}$ cluster. The

average charge contribution from s, p and d orbitals of Ge are in the ratio of 1.22:1.04:0.05, whereas, in Mo the ratio is 0.37:0.48:4.28. In $Ge_{12}Mo$ cage Mo atom gain about 4.0 electronic charges from the cage where average charge contribution from the Ge atoms is 0.34e, means the Mo atom behaves as a bigger charge receiver or as superatom. It enhances the electrostatic interaction between the cage and the Mo atom, which plays an important role in stabilizing $Ge_{12}Mo$ cage.

Similar information we obtained from the total density of states plot with s-, p-, d- site projected density of state contribution of Mo atom in different clusters in the size range n=10 to 14 and in different charged states (Electronic Supplementary Information Fig. 3SI). The PDOS is calculated using Mulliken population analysis. The DOS illustrates the presence of an electronic shell structure in $Ge_{12}Mo$ where the shapes of the single electron molecular orbitals (MOs) can be compared with the wave functions of a free electron in an spherically symmetric potential. The broadening in DOS occurs due to the high coordination of the central Mo atom. According to the phenomenological shell model in simple way assumes that the valence electrons in a cluster usually delocalized over the surface of the whole cluster whereas the nuclei and core electrons can be replaced by their effective mean-field potential. Therefore, the molecular orbitals (MOs) have the shape similar to those of the s, p, d, ... etc atomic orbitals which is labeled as S, P, D, ... etc.

TABLE 2: NATURAL ELECTRONIC CONFIGURATION (NEC) IN $Mo@Ge_{12}$

Atom	Orbital charge contribution			Total Charge	NEC
	s	p	d		
Ge	1.220	1.052	10.002	12.274	$3d^{1.220}4s^{1.052}4p^{10.002}$
Ge	1.218	1.057	10.002	12.277	$3d^{1.218}4s^{1.057}4p^{10.002}$
Ge	1.219	1.054	10.002	12.275	$3d^{1.219}4s^{1.054}4p^{10.002}$
Ge	1.219	1.053	10.002	12.274	$3d^{1.219}4s^{1.053}4p^{10.002}$
Ge	1.221	1.049	10.002	12.271	$3d^{1.221}4s^{1.049}4p^{10.002}$
Ge	1.217	1.058	10.002	12.277	$3d^{1.217}4s^{1.058}4p^{10.002}$
Ge	1.219	1.051	10.002	12.272	$3d^{1.219}4s^{1.051}4p^{10.002}$
Ge	1.221	1.046	10.001	12.268	$3d^{1.221}4s^{1.046}4p^{10.001}$
Ge	1.219	1.050	10.002	12.271	$3d^{1.219}4s^{1.050}4p^{10.002}$
Ge	1.219	1.053	10.002	12.273	$3d^{1.219}4s^{1.053}4p^{10.002}$
Ge	1.217	1.054	10.002	12.273	$3d^{1.217}4s^{1.054}4p^{10.002}$
Ge	1.221	1.045	10.001	12.268	$3d^{1.221}4s^{1.045}4p^{10.001}$
Mo	0.375	0.484	4.273	5.1320	$5s^{0.375}4p^{0.484}4d^{5.132}$

Enhanced stability of the clusters is expected if the number of delocalized electrons corresponds to a closed electronic shell structure. The sequence of the electronic shells depends on the shape of the confining potential. For

a spherical cluster with a square well potential, the orbital sequence is $1S^2$; $1P^6$; $1D^{10}$; $2S^2$; $1F^{14}$; $2P^6$; $1G^{18}$; $2D^{10}$; $1H^{22}$; ..., corresponding to shell closure at 2, 8, 18, 20, 34, 40, 58, 68, 90, ... roaming electrons. There are 54 valence electrons in $Ge_{12}Mo$. By comparison of the wave functions, the level sequence of the occupied electronic states in $Ge_{12}Mo$ can be described as $1S^2$; $1P^6$; $1D^8$ ($1D_I^8 + 1D_{II}^2$); $1F^{10}$ ($1F_I^6 + 1F_{II}^2 + 1F_{III}^2 + 1F_{IV}^2$); $2S^2$; $1G^2$; $2P^6$ ($2P_I^2 + 2P_{II}^4$); $3P^6$ ($3P_I^2 + 3P_{II}^2$) ; $2D^2$. Their positions in the DOS plot are shown in Fig. 3. Due to the crystal field splitting, which is related to the non-spherical or distorted spherical symmetry of the cluster some of the orbitals with higher angular momentum lifted up [39]. As example, 2P orbital of $Ge_{12}Mo$ cluster spitted into two as mentioned above. The most important difference with the energy level sequence of free electrons in a square well potential is the lowering of the 2D level. Examination of the 2D molecular orbitals show that they are mainly composed of the Mo 3d AOs, representing the strong hybridization between the central Mo with the Ge cage. The strong hybridization of the Mo 4d electrons with the Ge valence electrons (evidenced by the PDOS shown in Electronic Supplementary Information Figure 2SI) has implications for the quenching of magnetic moment of Mo. According to Hund' s rule, the electronic configuration in molybdenum is ([Kr] $5s^1$ $4d^5$). As per this arrangement Mo should pose a very high value of magnetic moment equal to 6 μB. The local magnetic moment of Mo in $Ge_{12}Mo$ is zero as well as in the all the ground state isomers (except ground states quintet Ge-Mo dimer and triplet Ge_2Mo). The quenched magnetic moment can be attributed to the charge transfer and the strong hybridization between the Mo 4d orbitals and Ge 4s, 4p orbitals. Mixing of d-orbital of transition metal is the main cause of stability enhancement in the cluster here. Though there is dominating contribution of Mo d-orbital in the $Ge_{12}Mo$ cluster, but close to the Fermi energy level hardly there is any DOS or any contribution from Mo d-orbital. This explains the presence of HOMO-LUMO gap in the cluster and less reactive nature of the cluster. This is also true for the ground state clusters for n=10 and 11. From the DOS picture, it is clear that for n=10, 11, 12 and 13 ground state clusters the HOMO-LUMO gap is comparable. The DOS of the anionic $Ge_{11}Mo$, which is an 18-electron cluster, show the presence of considerable fraction of DOS on the Fermi level. Therefore, there is a possibility for anionic $Ge_{11}Mo$ cluster to form a ligand and at the higher charged states by combining with other species it can make a more stabile species which is an indication of possibility of making cluster assembled materials. To get an idea how the magnetic moment of the clusters are changing and reducing to zero from Ge-Mo dimer with the increase of the cluster size, we have studied the site projected magnetic moment of the small sized neutral and cationic clusters (up to n=3) following the work reported by Hou et. al. [5]. The Ge-Ge dimer is in triplet state with ferromagnetic coupling between the germanium atoms

with total magnetic moment of $2\mu_B$. On the other hand, in Mo-Mo dimer, though the individual moment of the Mo atoms are very high, but the interaction between them is antiferromagnetic and hence the magnetic moment of Mo-dimer is reduces to zero. Detailed results of the variation of magnetic moments are given in Electronic Supplementary Information Fig. 1SIc. The ground states of neutral and cationic Ge-Mo dimers in quintet and quartet spin states with the magnetic moment of the clusters are 4μ and 3μ respectively. The interaction between the Ge-Mo in the ground state is antiferromagnetic with a bond length of $2.50A^0$. In the cationic cluster the bond length reduces to 2.67 A^0 with the presence of antiferromagnetic interactions between Ge and Mo. The same dimer, when it is in triplet and septet spin states, the magnetic interactions changes from antiferromagnetic to ferromagnetic, and the bond length changes from 2.34 A^0 to 2.73 A^0 respectively. Following the electronic configuration of 10 (4 from Ge and 6 from Mo) valance electrons (Triplet: $\boldsymbol{\sigma s^2}$ $\boldsymbol{\sigma s^2}$ πp^2 πp^2 $\boldsymbol{\sigma s^1}$ πp^1; Quintet: $\boldsymbol{\sigma s^2}$ $\boldsymbol{\sigma s^2}$ πp^2 πp^1 $\boldsymbol{\sigma s^1}$ πp^1 πp^1; Septet: $\boldsymbol{\sigma s^2}$ $\boldsymbol{\sigma s^2}$ πp^1 πp^1 $\boldsymbol{\sigma s^1}$ πp^1 πp^1 πp^1) and corresponding orbitals (Electronic Supplementary Information Fig. 1SId), it can be seen that while shifting from triplet to quintet state, a beta electron from πp^2 state shifted to α-πp^1 state, which is at much dipper position compare to the α-HOMO orbital. In the whole rearrangement of the orbitals due to this spin flip, the α-HOMO orbital of the triplet state move to α-HOMO orbital of quintet spin state with a small difference in energy of 0.08 eV with the same antiferromagnetic interaction between the two atomic spins. It is also important to mention that in quintet state, the local spin of Mo increases, whereas the same in Ge decreases compare to the spins in triplet state. Due to the transition from quintet to septet, the πp^1 (β-HOMO) shifted to α-HOMO of energy difference of 1.10 eV compare to the β-HOMO in quintet state. The magnetic interaction also changes from antiferromagnetic to ferromagnetic. In triplet and septet states, the optimized energies of the clusters are 0.25 eV and 0.57 eV respectively more compare to the quintet ground state. Hence the dimer Ge-Mo is found more stable in quintet spin state. Addition of one germanium atom to the Ge-Mo dimer, the ground state found is in triplet spin state. In Ge_2Mo ground state cluster in triplet spin state the interactions between the Mo and the two-germanium atoms are antiferromagnetic with the spin magnetic moments $3.34\mu_B$, $-0.67\mu_B$ and $-0.67\mu_B$ respectively and with different bond lengths (Electronic Supplementary Information Fig.1SIc). Due to the antiferromagnetic bonding between the Mo and two Ge atoms, the magnetic moment reduces to 2 μ_B in Ge_2Mo ground state cluster. The two-germanium atoms are connected by π-bonding as shown in the filled α-HOMO orbital (Electronic Supplementary Information Fig. 1SId). The other two low energy clusters are in singlet spin states. From the electronic

configuration of 14 (4 from each Ge atoms and 6 from Mo) valance electrons (Triplet: $(3a_1)^2$ $2(b_2)^2$ $4(a_1)^2$ $2(b_1)^2$ $5(a_1)^2$ $1(a_2)^2$ $3(b_2)^1$ $6(a_1)^1$; Quintet: $(3a_1)^2$ $2(b_2)^2$ $4(a_1)^2$ $2(b_1)^2$ $5(a_1)^2$ $1(a_2)^1$ $3(b_2)^1$ $6(a_1)^1$ $3(b_1)^1$) and corresponding orbitals (Electronic Supplementary Information Fig. 1SId) in Ge_2Mo it can be seen that the β-HOMO electron from $1(a_2)^2$ in triplet state transferred to α-HOMO in quintet spin state of Ge_2Mo cluster which is at +0.93eV higher compare to triplet α-HOMO level. During this transition the overall ground state energy change is +0.56 eV. Therefore, addition of one Ge atom with the Ge-Mo dimer in quintet state reduces the magnetic moment and as a result the Ge_2Mo cluster in triplet spin state is the ground state. It is also interesting to study the charge or the orbitals distributions in β-HOMO triplet and α-HOMO quintet of Ge_2Mo cluster. The orbital distributions indicating the presence of electron distributions along the bond between the Ge-Mo dimers and hence the bonding nature is strong and therefore the spin magnetic moment of Mo reduces to $3.34\mu_B$. In the same state, the hardly there is any orbital distributions along Ge-Ge bond. When it switches in the septet state, the bonding between Ge-Mo has increased and reduced in Ge-Ge. Therefore the spin of Mo has increased. The magnetic moment vanishes in Ge_3Mo ground state cluster completely with no non-zero onsite spin values of the atoms. With reference to the work reported by Khanna et. al. [40], when a 3d transition atoms makes bond with Si cluster in a Si_nTM, there always exists a strong hybridization between the 3d of the TM with 3s3p of Si atoms. The present investigation as discussed above following the same as reported by Khanna et. al [40] and is one of the strongest evidence of the quenching of spin magnetic moment of Mo atom. The strong hybridization between $4d^5$ of Mo with the $4s^24p^2$ of Ge atom, the magnetic moment of Mo quenched with no left over part to hold its spin moment in Ge_3Mo ground state cluster. In this contest it is also worth to mention the work of Janssens et. al. [41] on the quenching of magnetic moment of Mn in Ag_{10} cage where they suggested that the valance electrons of silver atoms in the cage can be considered as forming a spin-compensating electron cloud surrounding the magnetic impurity which is conceptually very much similar to Kondo effect in larger system and may be applied in our system also.

To get the idea about the kinetic stability of the clusters in chemical reactions the HOMO-LUMO gap (ΔE), ionization potential (IP), electron affinity (EA), chemical potential (μ), chemical hardness (η) are calculated. In general with the increase of HOMO-LUMO gap the reactivity of the cluster decreases. Variation of HOMO-LUMO gaps of neutral and cationic $Mo@Ge_n$ clusters is plotted and is shown in the Electronic Supplementary Information Fig. 4SI. The variation of HOMO-LUMO gap is oscillatory. Overall there is a large variation in HOMO-LUMO gap

in the whole size range between 1.5 to 3.30 eV with a local maxima at n=12 and at n=13 in neutral and cationic clusters respectively. This is again an indication of enhance stability of 18-electron clusters. The large HOMO-LUMO gap (2.25 eV) of $Mo@Ge_{12}$ could make this cluster as a possible candidate as luminescent material in the blue region. In the neutral state the sizes n=8, 10, 12, 14, 18 are magic in nature, means a higher relative stability. Variation of HOMO-LUMO gap in different clusters around the Fermi level can be useful as device applications. The variation of ionization energy shown in Fig. 2a with a sharp peak at n=12 with a value of 7.16 eV as like other parameters supports the higher stability of $Ge_{12}Mo$ cluster. According to the electron shell model, whenever a new shell starts filling for the first time, its IP drops sharply. De Heer [42] has reported that in Li_n series, L_{20} cluster is a shell field configuration and there is a sharp drop in IP when the cluster grows from L_{20} to L_{21}. This is one of the most important evidence to support $Ge_{12}Mo$ as a 18-electron cluster. There is a local peak in the IP graph at n=12, followed by a sharp drop in IP at n=13. The drop in IP could be the strongest indication of the assumption of nearly free-electron gas inside the $Ge_{12}Mo$ cage cluster. Following the other parameters, one may demand that the $Ge_{14}Mo$ cluster is following the 20-electron counting rule. But we did not accept it, because the IP at n=14 does not show local maxima. From the above discussion, it is clear that the neutral hexagonal D_{6h} structure of $Ge_{12}Mo$ with a large fragmentation energy, averaged atomic binding energy and IP is suitable as the new building block of self assembled cluster materials. This is reflecting that the stability of the pure germanium cluster is obviously strengthened when the Mo atom is enclosed in its Ge_n frames. Hence it can be expected that the enhanced stability of $Mo@Ge_{12}$ makes a contribution toward the initial model to develop a new type of Mo doped germanium superatom as well as Mo-Ge based cluster assembled materials. Further, to verify the chemical stability of Ge_nMo clusters, chemical potential (μ) and chemical hardness (η) of the ground state isomers are calculated. In practice chemical potential and chemical hardness can be expressed in terms of electron affinity (EA) and ionization potential (IP). In terms of total energy consideration if E_n is the energy of the n electron system, then energy of the system containing $n+\Delta n$ electrons where $\Delta n << n$ can be expressed as:

$$E_{n+\Delta n} = E_n + \left.\frac{dE}{dx}\right|_{x=n} \Delta n + \frac{1}{2}\left.\frac{d^2E}{dx^2}\right|_{x=n} (\Delta n)^2 + \textit{Neglected higher order terms}$$

Then, μ and η can be defined as:

$$\mu = \left.\frac{dE}{dx}\right|_{x=n} \text{ and } \quad \eta = \frac{1}{2}\left.\frac{d^2E}{dx^2}\right|_{x=n} = \frac{1}{2}\left.\frac{d\mu}{dx}\right|_{x=n}$$

Since, $IP = E_{n-1} - E_n$ and $EA = E_n - E_{n+1}$.

By setting $\Delta n = 1$, μ and η are related to IP and EA via the following relations:

$$\mu = -\frac{IP + EA}{2} \text{ and } \eta = \frac{IP - EA}{2}$$

Now for consider two interacting systems with μ_i and η_i (i=1,2) where some amount of electronic charge (Δq) transfers from one to other. The quantity Δq and the resultant energy change (ΔE) due to the charge transfer can be determined in the following way:

If $E_{n+\Delta q}$ is the energy of the system after charge transfer then it can be expressed for the two different systems 1 and 2 in the following way:

$$E_{1\,n_1+\Delta q} = E_{1\,n_1} + \mu_1(\Delta q) + \eta_1(\Delta q)^2$$

and $E_{2\,n_2-\Delta q} = E_{2\,n_2} - \mu_2(\Delta q) + \eta_2(\Delta q)^2$

Corresponding chemical potential becomes,

$\mu_1' = \left.\frac{dE_{1\,x+\Delta q}}{dx}\right|_{x=n_1} = \mu_1 + 2\eta_1\Delta q$ and $\mu_2' = \left.\frac{dE_{2\;x-\Delta q}}{dx}\right|_{x=n_2} = \mu_2 - 2\eta_2\Delta q$ to first order in ΔM after the charge transfer. In chemical equilibrium, $\mu_1' = \mu_2'$ which gives the following expressions:

$$\Delta q = \frac{\mu_2 - \mu_1}{2(\eta_1 + \eta_2)} \text{ and } \Delta E = \frac{(\mu_2 - \mu_1)^2}{2(\eta_1 + \eta_2)}$$

In the expression, energy gains by the total system (1 and 2) due to exclusive alignment of chemical potential of the two systems at the same value. From the above expressions that for easier charge transfer from one system to other it

is necessary to have a large difference in μ together with low η_1 and η_2. Therefore, Δq and ΔE can be taken as the measuring factors to get the idea about the reaction affinity between two systems. Since they are function of the chemical potential and chemical hardness related to the system, so it is important to calculate these parameters of a system to know about its chemical stabilities in a particular environment. Keeping these in mind, chemical potential (μ) and chemical hardness (η) for Mo doped Ge_n clusters is calculated. Dip at n=12 in chemical potential plot (Fig. 4a) is actually indicating stable chemical species, hence low affinity of the system to take part in chemical reaction in a particular environment. Again at n=12, the presence of a local peak in chemical hardness plot is also supporting the result of low chemical affection $Mo@Ge_{12}$ cluster. The ratio of these two parameters in positive sense shows a peak and hence indicating the low chemical affinity. Since n=12 is a 18-electron cluster, it is clear that this cluster also show low affinity in chemical reaction and is in stability agreement with the other parameters.

4. POLARIZABIILITY

It is known that the static polarizability is a measure of the distortion of the electronic density and sensitive to the delocalization of valance electrons [43]. Hence it is the measure of asymmetry in three-dimensional structures and orbital distributions. It gives the information about the response of the system under the effect of an external electrostatic electric field. The average static polarizability is defined as:

$$\langle \alpha \rangle = \frac{1}{3}\left(\alpha_{XX} + \alpha_{YY} + \alpha_{ZZ}\right)$$

in terms of principle axis, which is a function of basis set, used in the optimization of the clusters [44, 45]. In the current work, the variation of polarizability and the electrostatic dipole moment of the clusters are shown in Fig. 4b. As exhibited in Fig. 4b, one can find that the polarizability of the cluster increase as a function of the cluster size 'n' which is nearly linear with local dip at n=12. At this size the electrostatic dipole moment is also minimum. This trend of variation of polarizability with the cluster size for $Mo@Ge_n$ clusters is similar to the water clusters reported by Ghanty and Ghosh [45].

5. NUCLEUS-INDEPENDENT CHEMICAL SHIFT (NICS)

The most widely employed method to analyze the aromaticity of different species is the NICS index descriptor proposed by Schleyer et. al. [46]. NICS index is defined as the negative value of the absolute shielding computed at

a ring center or at some other point of the system which can describe the system nicely, as example, the symmetry point like the center of a hexagon. The rings with more negative NICS values are considered as more aromatic species. On the other hand, zero (or close to zero) and positive NICS values are indicative of non-aromatic and anti-aromatic species. NICS is usually computed at ring centers or at a distance on both side of the ring center. NICS obtained at 1Å above the molecular plane [47] is usually considered to better reflect the p-electron effects than NICS(0). Since we are interested to study the aromaticity of the overall ground state isomer $Mo@Ge_{12}$, which is hexagonal prism like structure with Mo, doped at the center, we have measured NICS values at the position of Mo and then along the symmetry axis perpendicular to the hexagonal plane surface. The NICS calculations have been performed based on the magnetic shielding using GIAO-B3LYP level of theory by placing a ghost atom at certain points along the symmetry axis. Variation of NICS value with the distance from the center of the system is shown in Fig. 5. Nature of the variation of NICS indicates the aromatic behavior of the cluster with a maximum negative value of -96.033 ppm at the center of the hexagonal surface and with a distance 1.5Å from the center of the cluster. Aromaticity of hexagonal structures (like benzene) is an important conformation of its stability. Therefore, in the present calculations the NICS behavior of $Mo@Ge_{12}$ also supports the stability of the cluster.

CONCLUSION

In summary, a report on the study of geometry and electronic properties of neutral and cationic Mo-doped Gen (n =1-20) clusters within the framework of density functional theory is presented. Identification of the stable species, and variation of chemical properties with the size $Mo@Ge_n$ clusters will helps to understand the science of Ge-Mo based clusters and superatoms that can be future building blocks for cluster-assembled designer materials and could open up a new field in electronic industry. The present work is the preliminary step in this direction and will be followed by more detailed studies on these systems in near future. On the basis of the results, the following conclusions have been drawn.

1. The growth pattern of Ge_nMo clusters can be grouped mainly into two categories. In the smaller size range i.e. before encapsulation of Mo atom, Mo or Ge atoms are directly added to the Ge_n or $Ge_{n-1}Mo$ respectively to form Ge_nMo clusters. At the early part in this region the binding energy of the clusters increase in a much faster rate than the bigger clusters. After encapsulation of Mo atom by the Ge_n cluster for n>9, the size of the Ge_nMo clusters tend to increase by absorbing Ge atoms one by one on its surface keeping Mo atom inside the cage.

2. It is favorable to attach a Mo-atom to germanium clusters at all sizes, as the EE turns out to be positive in every case. Clusters containing more than nine germanium atoms are able to absorb Mo atom endohedrally in a germanium cage both in pure and cationic states. In all Mo-doped clusters beyond n > 2, the spin magnetic moment on the Mo atom is quenched in expenses of stability. As measured by the BE, EE, HOMO-LUMO gap, FE, stability and other parameters both for neutral and cationic clusters, it is found that those are having 18 valence electrons show enhanced stability which is in agreement with shell model predictions. This also shows up in the IP values of the Ge_nMo clusters, as there is a sharp drop in IP when cluster size changes from n=12 to 13. Validity of nearly free-electron shell model is similar to that of transition metal doped silicon clusters. Although the signature of stability is not so sharp in the HOMO-LUMO gaps of these clusters, there is still a local maximum at n=12 for the neutral clusters, indicating enhanced stability of a 18-electron cluster, whereas, this signature is very much clear in cationic $Ge_{13}Mo$ cluster. Variation in HOMO-LUMO gap in different sized clusters could be useful for devise applications. The large HOMO-LUMO gap (2.25 eV) of $Mo@Ge_{12}$ could make this cluster as a possible candidate as luminescent material in the blue region.

3. Major contribution of the charge from the d-orbital of Mo in hybridization and its dominating contribution in DOS indicate that the d-orbitals of Mo atoms are mainly responsible in the hybridization and stability of the cluster. Presence of the dominating contribution of Mo d-orbital close to the Fermi level in DOS is also significant for ligand formation and a strong indication of possibility to make stable cluster assembled materials.

4. Computations and detailed orbital analysis of the clusters confirmed the rapid quenching of the magnetic moment of Mo in Ge_n host cluster while increasing the size from n=1 to 3. Beyond n=2, all hybrid clusters are in singlet state with zero magnetic moment. Following the overall shape of the delocalized molecular orbitals of $Ge_{12}Mo$ (Fig. 3) cage like clusters, the valance electrons of Ge_{12} cage can be considered as forming a spin compensating electron cloud surrounding the magnetic element Mo as like a screening electron cloud surrounding Mo which is similar to the magnetic element doped bulk materials. Therefore, the system may be interpreted as very similar to that of a finite-size Kondo system.

5. Variation of calculated NICS values with the distance from the center of the cluster clearly indicates that the cluster is aromatic in nature and the aromaticity of the cluster is one of the main reasons for its stability.

ELECTRONIC SUPPLEMENTARY INFORMATIONS

Electronic Supplementary Information includes the calculated low energy isomers, variation of different thermodynamic parameters with the cluster size, DOS, results of additional calculations using M06 functional, details of bonding and anti-bonding in small sized clusters obtained from the Gaussian outputs.

ACKNOLEDGEMENTS

R.T., K.D. and D.B. are gratefully acknowledge Dr. Biman Bandyopadhyay, Department of Chemistry, IEM, Kolkata, INDIA for valuable discussions. A part of the calculation is done at the cluster computing facility, Harish-Chandra Research Institute, Allahabad, UP, India (http://www.hri.res.in/cluster/).

REFERENCES

1. K. Sattler, ed. *Cluster assembled materials*., CRC Press, 1996, vol. 232.

2. V. Kumar and Y. Kawazoe, *Applied Physics Letters*, 2001, **5**, 80.

3. G. Gopakumar, X. Wang, L. Lin, J.D. Haeck, P. Lievens and M.T. Nguyen, *The Journal of Physical Chemistry C,* 2009, **113**, 10858.

4. G. Gopakumar, P. Lievens and M.T. Nguyen, *The Journal of Physical Chemistry A*, 2007, **111**, 4353.

5. X. J. Hou, G. Gopakumar, P. Lievens and M.T. Nguyen, *The Journal of Physical Chemistry A*, 2007, **111**, 13544.

6. V.T. Ngan, J. De Haeck, H.T. Le, G. Gopakumar, P. Lievens and M.T. Nguyen, *The Journal of Physical Chemistry A*, 2009, **113**, 9080.

7. D. Bandyopadhyay, *Journal of Applied Physics*, 2008, **104**, 084308.

8. D. Bandyopadhyay, *Molecular Simulation*, 2009, **35**, 381.

9. D. Bandyopadhyay, *Journal of molecular modeling*, 2012, **18**, 737.

10. D. Bandyopadhyay and P. Sen, *The Journal of Physical Chemistry A*, 2010, **114**, 1835.

11. D. Bandyopadhyay, M. Kumar, *Chemical Physics,* **353**, 170.

12. S. M. Beck, *Journal of Chemical Physics*, 1987, **87**, 4233.

13. S. M. Beck, *Journal of Chemical Physics*, 1989, **90**, 6306.

14. J. Atobe, K. Koyasu, S. Furuseand and A. Nakajima , *Physical Chemistry Chemical Phys*ics 2012 **14**, 9403

15. H. Hiura, T. Miyazaki and T. Kanayama, *Physical Review Letters,* 2001, **86**, 1733

16. J. Wang and J. G. Han, *Chemical Physics*, 2007, **342**, 253.

17. L. J. Guo, G. F. Zhao, Y. Z. Gu, X. Liu and Z. Zeng , *Physical Review B*, 2008, **77**, 195417

18. J. U. Reveles and S. N. Khanna, *Physical Review B,* 2005, **72**, 16513

19. E. Wigner and E. E. Witmer, *Z. Phys*, 1928,. **51**, 859

20. K. Koyasu, M. Akutsu, M. Mitsui and A. Nakajima, *Journal of American Chemical Society*, 2005, **127**, 4998

21. C. Lee, W. Yang and R. G. Parr, *Physical Review B*, 1988, **37**, 785; J. P. Perdew, *Physical Review B*, 1996, **54,** 16533.

22. M. J. Frisch, G. W. Trucks, H. B. Schlegel, G. E. Scuseria, M. A. Robb, J. R. Cheeseman, V. G. Zakrzewski, Jr J. A. Montgomery, R. E. Stratmann, J. C. Burant, S. Dapprich, J. M. Millam, A. D. Daniels, K. N. Kudin, M. C. Strain, O. Farkas, J. Tomasi, V. Barone, M. Cossi, B. C. Mennucci, C. Pomelli, C. Adamo, S. Clifford, J. Ochterski,

G. A. Petersson, P. Y. Ayala, Q. Cui, K. Morokuma, D. K. Malick, A. D. Rabuck, K. Raghavachari, J. B. Foresman, J. Cioslowski, J. V. Ortiz, A. G. Baboul, B. B. Stefanov, B. Liu, A. Liashenko, P. Piskorz, I. Komaromi, R. Gomperts, R.L. Martin, D. J. Fox, T. Keith, M. A. Al-Laham, C. Y. Peng, A. Nanayakkara, M. Challacombe, P. M. W. Gill, B. Johnson, W. Chen, M. W. Wong, J. L. Andres, C. Gonzalez, M. Head-Gordon, E. S. Replogle, J. A. Pople, GAUSSIAN 03(Revision E.01) Gaussian Inc., Wallingford, 2004

23. P. J. Hay and W. R. Wadt, *Journal of Chemical Physics,* 1985, **82**, 270.

24. P. J. Hay, W. R. Wadt, *Journal of Chemical Physics*, 1985, **82**, 284; P. J. Hay and W. R. Wadt, *Journal of Chemical Physics,* 1985, **82**, 299.

25. C. W. Glass, A. R. Oganov and N. Hansen, *Computer Physics Communications*, 2006, **175**, 713.

26. G. Kresse and J. Furthmüller, *Physical Review B*, 1996, **54**, 11169 .

27. G. Kresse and D. Joubert, *Physical Review B*, 1999, **59**, 1758.

28. E. Northrup and M. L. Cohen, *Chemical Physical Lett*ers, 1983, **102**, 440.

29. T. A. Abtew and D. A. Darbold, *Physical Review B*, 2007, **75**, 145201.

30. J. Wang and J. G. Han, *The Journal of Physical Chemistry A,* 2006, **110**, 12670.

31. J. Wang and J. G. Han, *The Journal of Physical Chemistry A*, 2008, **112***,* 3224.

32. J. R. Lombardi and B. Davis, *Chemical Review*, 2002, **102**, 2431.

33. W. Kohn and L. Sham, *Journal of Physical Review*, 1965, **140**, A1133.

34. T. B. Tai and M. T. Nguyen, *J. Chem. Theo. Commun*, 2011, **7**, 1119

35. K. Dhaka, R. Trivedi and D. Bandyopadhyay, *Journal of Molecular Modeling,* 2013, **19**, 1437.

36. M. Kumar, N. Bhattacharya and D. Bandyopadhyay, *Journal of Molecular Modeling,* 2012, **18**, 405.

37. D. Bandyopadhyay, P. Kaur and P. Sen, *The Journal of Physical Chemistry A*, 2010, **114**, 12986.

38. D. Bandyopadhyay, *Journal of Molecular Modeling,* 2012, **18**, 3887.

39. Y. Li, N. M. Tam, P. Claes, A. P. Woodham, J. T. Lyon, V. T. Ngan, M. T. Nguyen, P. Lievens, A. Fielicke and E. Janssens, *The Journal of Physical Chemistry A,* 2014, **118**, 8198.

40. S. N. Khanna, B. K. Rao, P. Jena, *Physical Review Letters*, 2002, **89**, 016803.

41. E. Janssens, S. Neukermans, H.M.T. Nguyen, M.T. Nguyen and P. Lievens, *Physical Review Letters,* 2005, **94**, 113405

42. W. A. de Heer, *Reviews of Modern Physics*, 1993, **65**, 611

43. Y. R. Zhao, X. Y. Kuang, B. B. Zheng, Y. Fang and S. J. Wang, *The Journal of Physical Chemistry A,* 2011, **115**, 569

44. T. K. Ghanty and S. K. J. Ghosh, *Chemical Physics,* 2003, **118**, 8547.

45. T. K. Ghanty and S. K. J. Ghosh, *Physical Chemistry*, 1996, **100**, 17429.

46. P. Schleyer, R. van, C. Maerker, A. Dransfeld, H. Jiao and N. J. R. E. Hommes, *Journal of American Chemical Society*, 1996, **118**, 6317

47. A. E. Kuznetsov and A. I. Boldyrev, *Chemical Physical Letters*, 2004, **388**, 452.

List of Figures:

List of Tables:

Fig. 1. Variation of average binding energy per atom of the clusters with the cluster size (n).

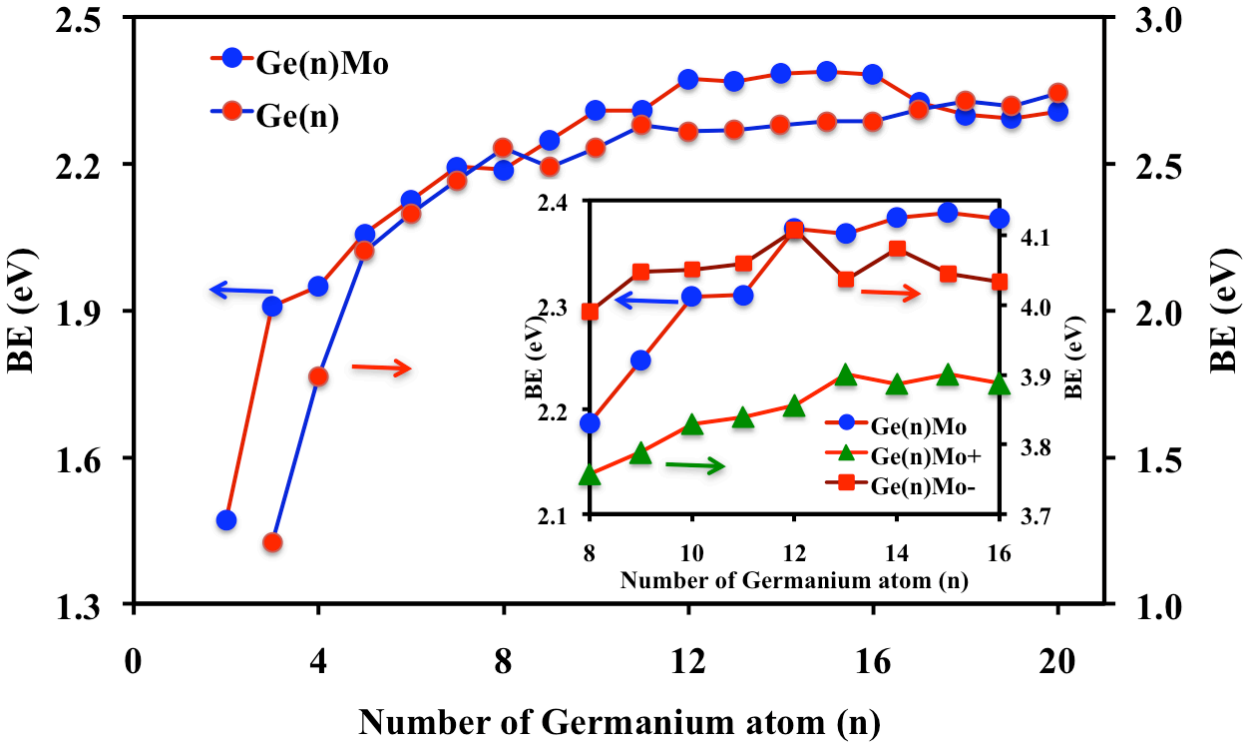

Fig. 2. Variation of (a) Embedding Energy (EE) and ionization potential (IP), (b) Stability, (c) Fragmentation Energy (FE) of neutral and cationic Mo@Ge_n clusters with the cluster size (n)

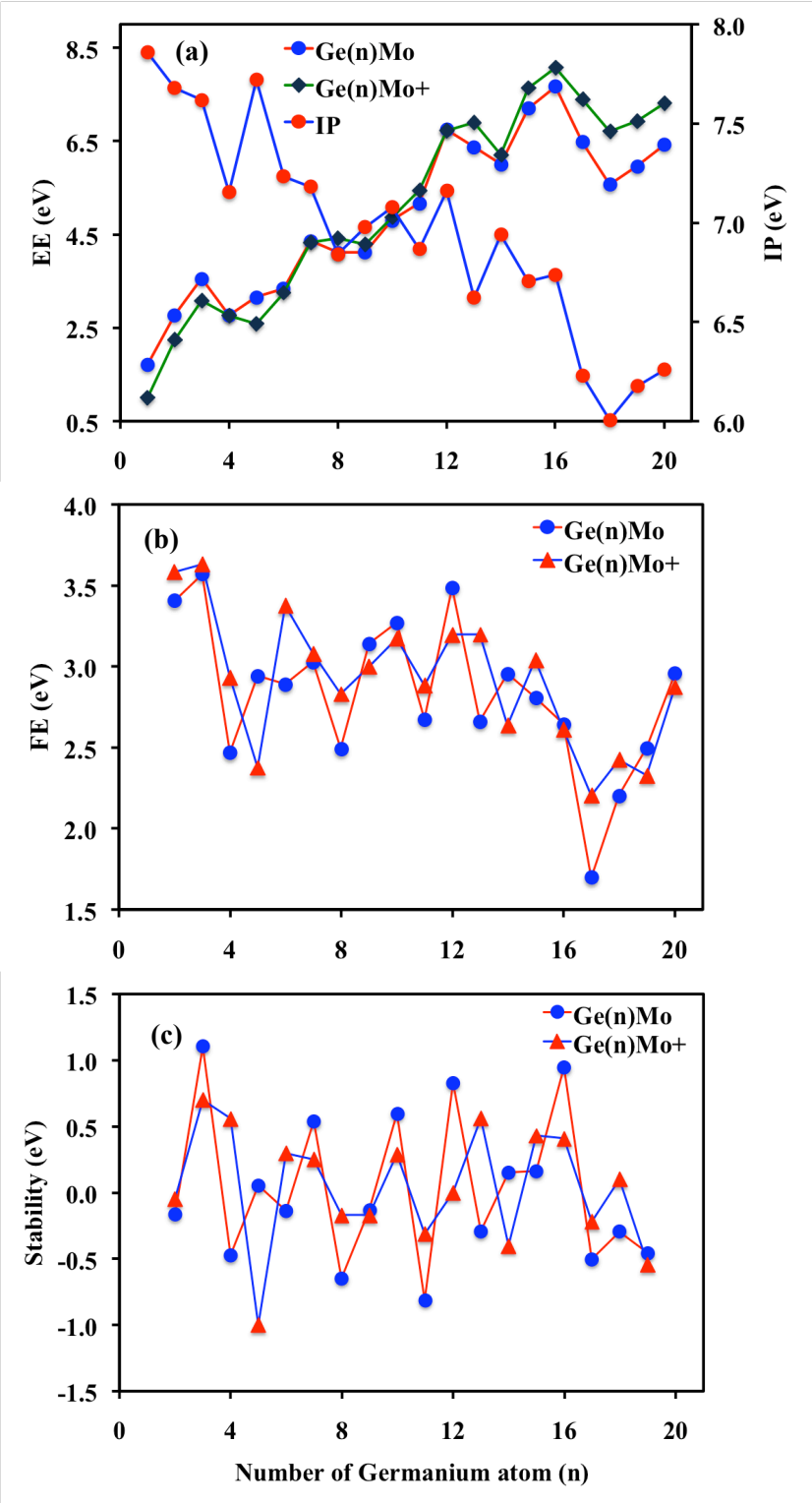

Fig.3. Density of State of $Ge_{12}Mo$ and its different orbitals with their position in DOS.

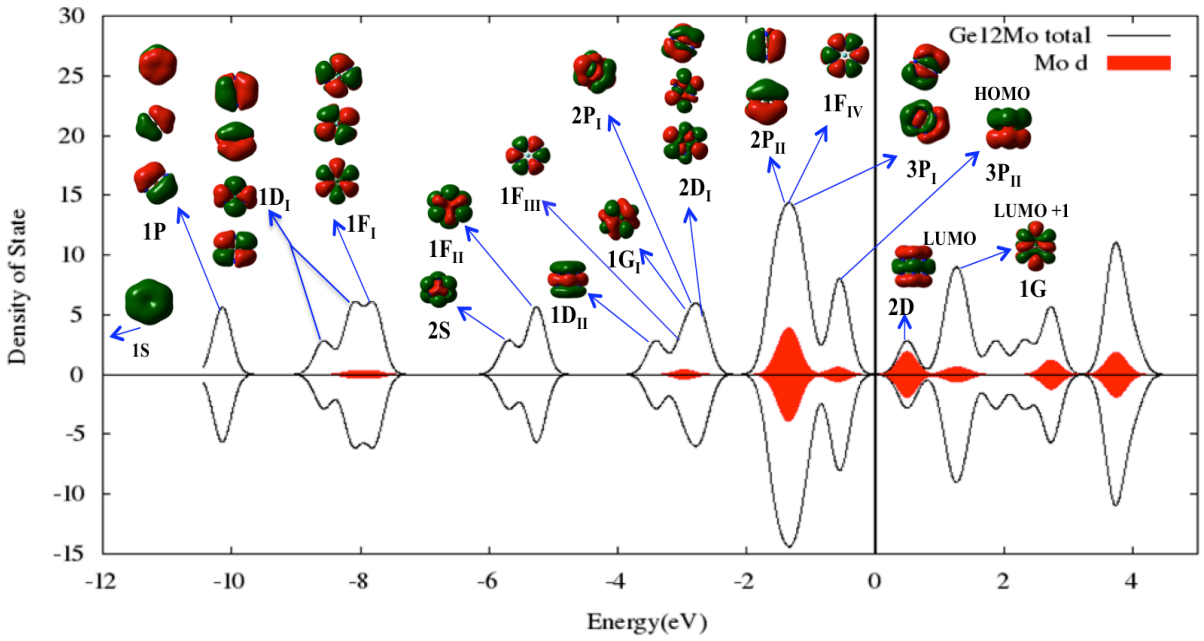

Fig. 4. Variation of (a) chemical potential and chemical hardness, (b) polarizability (Bhor**3) and electrostatic dipole moments of $Mo@Ge_n$ clusters with the cluster size.

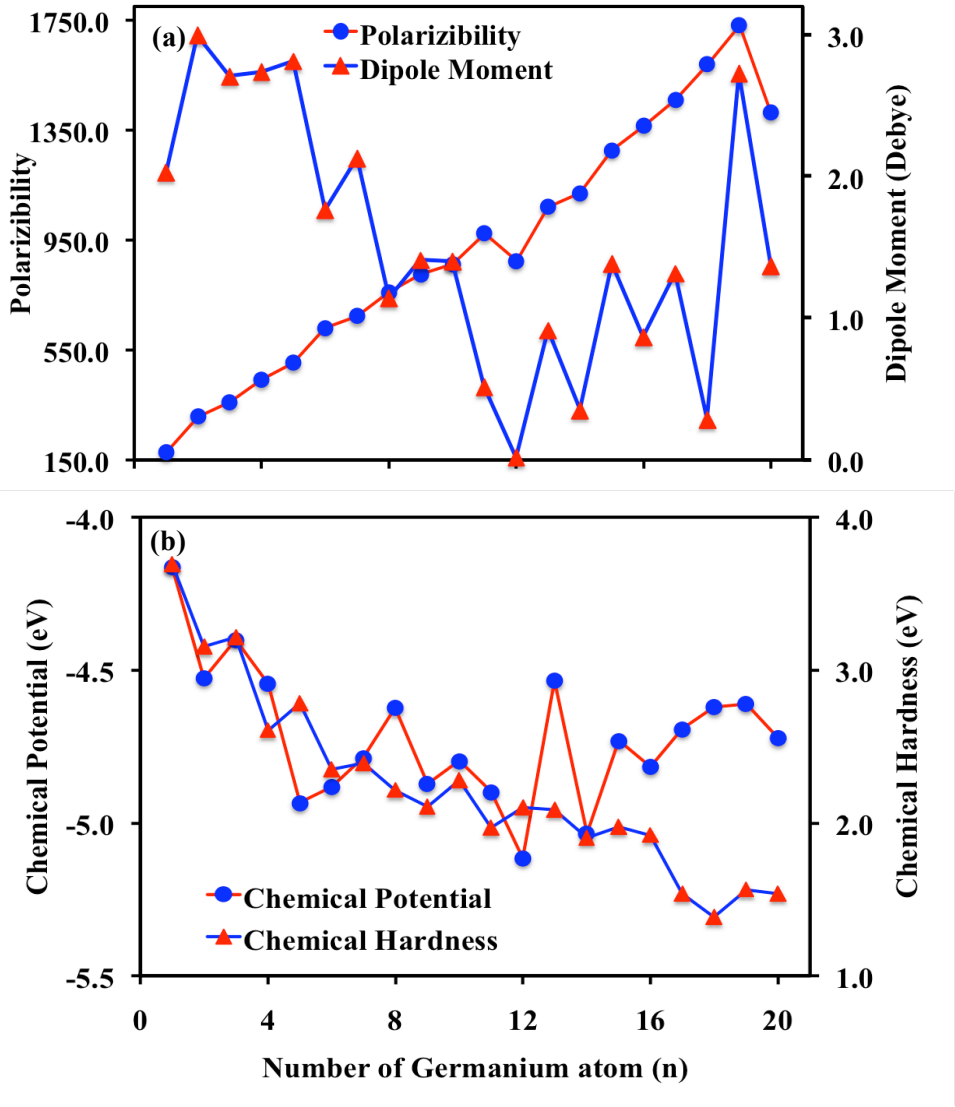

Fig. 5. NICS plot of $Mo@Ge_{12}$ cluster